Cellular Signalling 61 (2019) 1–9

Contents lists available at ScienceDirect

Cellular Signalling

journal homepage: www.elsevier.com/locate/cellsig

BCL-XL directly retrotranslocates the monomeric BAK

Bin Wang[a], Zihao Mai[a], Mengyan Du[a], Lu Wang[a], Fangfang Yang[a], Yunyun Ma[a], Xiaoping Wang[b,*], Tongsheng Chen[a,*]

[a] MOE Key Laboratory of Laser Life Science & College of Biophotonics, South China Normal University, Guangzhou 510631, China
[b] Department of Pain Management, the First Affiliated Hospital, Jinan University, Guangzhou 510632, China

ARTICLE INFO

Keywords:
BCL-XL
BAK
Apoptosis
Retrotranslocation
FRET
FLIP

ABSTRACT

BCL-XL, an anti-apoptotic BCL-2 family protein, potently inhibits BAK oligomerization and the formation of toxic mitochondrial pores in response to cellular stress. This report aims to explore which form of mitochondrial monomeric and oligomerized BAK can be retrotranslocated by BCL-XL. Fluorescence imaging of living cells co-expressing CFP-BCL-XL and YFP-BAK showed that BCL-XL markedly inhibited mitochondrial BAK oligomerization and resulted in partial cytosolic BAK distribution. Live-cell fluorescence resonance energy transfer (FRET) analyses showed that BAK auto-oligomerized on mitochondria and BCL-XL physically sequestrated monomeric BAK to prevent BAK oligomerization. Fluorescence loss in photobleaching (FLIP) analyses showed that BCL-XL retrotranslocated the monomeric BAK from mitochondria into cytosol, whereas monomeric BAK reduced the retrotranslocation rate of BCL-XL. Live-cell time-lapse imaging and FLIP experiments in living cells with BAK oligomers displayed that BCL-XL did not depolymerize or retrotranslocate the oligomerized BAK. Collectively, BCL-XL retrotranslocates monomeric instead of oligomerized BAK from mitochondria into cytosol.

1. Introduction

BAK and BAX, two pro-apoptotic BCL-2 proteins, are central controllers in apoptosis [1,2]. When cells suffer apoptotic stimulus, BAK and BAX are activated and then oligomerize on mitochondrial outer membrane (MOM) to permeabilize MOM via forming pores [3–5], releasing mitochondrial cytochrome *c* (cyt c) and other apoptotic factors into cytosol to initiate the caspase cascade that causes cell death [6–9]. BAX, predominantly in cytosol in healthy cells, translocates and accumulates in MOM before oligomerization during apoptosis, while BAK, an integral MOM protein, oligomerizes immediately bypassing the translocation step, thus possesses faster killing kinetics than BAX [10,11]. Moreover, recent studies reveal that BAK is involved in BAX translocation and oligomerization, whereas BAX is not essential for BAK oligomerization [12–14].

Prevention of BAK oligomerization is a pivotal step toward protecting cells survival [15,16]. The anti-apoptotic BCL-2 proteins (e.g. BCL-2, BCL-XL and MCL-1) play fundamental roles in preventing BAK oligomerization through sequestrating BH-3-only protein activators (e.g. BID and BIM) [17–19] or active BAK [20–22]. Furthermore, inactivation or downregulation of anti-apoptotic BCL-2 proteins results in BAK auto-activation even without activators [23,24]. BCL-XL is superior to BCL-2 and MCL-1 in resisting apoptosis [23]. Meanwhile, physiological restraint of BAK by BCL-XL has also been proven to be essential for cell survival [25]. On the other hand, BCL-XL effectively inhibits the pro-apoptotic function of BAK by retrotranslocating BAK from mitochondria into cytosol continuously, like BAX, even though BAK commonly anchors in MOM [26,27]. In addition, it was reported that the assembly pathway of BAK was a reversible process [28]. These findings hint a query that whether BCL-XL depolymerizes and retrotranslocates the oligomerized BAK from mitochondria into cytosol to inhibit the pro-apoptotic action of BAK.

This report utilized live-cell fluorescence imaging to explore the retrotranslocation of mitochondrial monomeric and oligomerized BAK by BCL-XL. Live-cell fluorescence resonance energy transfer (FRET) analyses demonstrated the oligomerization of mitochondrial BAK and the direct sequestration of monomeric BAK by BCL-XL. Fluorescence loss in photobleaching (FLIP) analyses showed that BCL-XL retrotranslocated the monomeric BAK from mitochondria into cytosol, whereas monomeric BAK reduced the retrotranslocation rate of BCL-XL.

Abbreviations: MOM, mitochondrial outer membrane; cyt c, cytochrome *c*; FRET, fluorescence resonance energy transfer; FLIP, fluorescence loss in photobleaching; I_{DD}, donor imaging; I_{AA}, acceptor imaging; I_{DA}, FRET imaging; E_A, acceptor-centric FRET efficiency; E_D, donor-centric FRET efficiency; R_C, concentration ratio; CV, Coefficient of Variation; DKO, $BAX^{-/-}BAK^{-/-}$

* Corresponding authors.
E-mail addresses: txp2938@jnu.edu.cn (X. Wang), chentsh@scnu.edu.cn (T. Chen).

https://doi.org/10.1016/j.cellsig.2019.05.001
Received 27 January 2019; Received in revised form 2 May 2019; Accepted 2 May 2019
Available online 03 May 2019
0898-6568/

Furthermore, live-cell time-lapse imaging and FLIP experiments displayed that BCL-XL inhibited BAK oligomerization on mitochondria but did not depolymerize and retrotranslocate the oligomerized BAK, indicating that BCL-XL prevents the formation of BAK oligomers by directly restraining and retrotranslocating the monomeric BAK.

2. Material and methods

2.1. Plasmids

CFP-BCL-XL was kindly provided by A. P. Gilmore [29]. ECFP-BAK (#31501), pcDNA3-CFP (CFP) (#13030) and pcDNA3-YFP (YFP) (#13033) plasmids were purchased from Addgene. Full-length BAK was synthesized by a standard PCR using ECFP-BAK as template for YFP-BAK plasmid and was cloned into the plasmid of pEYFP-C1-Drp1 (Addgene, #45160) by double enzyme digestion (*Xho*I and BamHI).

2.2. Cell culture and transfection

Hela cells obtained from the Department of Medicine, Jinan University (Guangzhou, China) were cultured just as described previously [30]. When cells reached 70% to 90% confluence in a 35-mm glass dish, plasmids were transfected into cells using Turbofect Transfection Reagent (Thermo Scientific) in the presence or absence of 50 μM *Z*-VAD-FMK (MedChemExpress). Co-transfection with 3-fold BCL-XL than BAK was performed.

2.3. Fluorescence imaging

Cells were washed in PBS, fixed with 4% paraformaldehyde in PBS for 10 min, permeabilized with 0.1% Triton X-100 in PBS for 10 min, and blocked in 5% BSA in PBS for 1 h, followed by incubation with appropriate primary anti-Tom20 (Cell Signaling Technology, #42406) in 5% BSA solution for 1 h, and probed with an Alexa-568-conjugated secondary antibody (Thermo Scientific). Confocal imaging was performed on a confocal microscope (Zeiss LSM 880, Germany) with Airyscan.

Cells were incubated with culture medium of Hoechst 33258 (G-clone, #CS2307) or DiIC1(5) (Thermo Scientific) according to the manufacture's protocol in the presence or absence of 50 μM *Z*-VAD-FMK. Fluorescence imaging was performed on a confocal microscope (Zeiss LSM 880, Germany) or a wide-field microscope (Olympus IX73 equipped with a CCD camera, Japan).

2.4. Quantitative FRET measurement

Quantitative FRET measurements were performed on an inverted wide-field fluorescence microscope (ApoTom.2, Carl Zeiss, Oberkochen, Germany) equipped with a 63 × 1.4 NA oil immersion lens and a CCD camera (Axiocam 506 mono, Carl Zeiss, Oberkochen, Germany). A cube comprising a BP436/20 excitation filter (Carl Zeiss, Germany) and a dichroic mirror of DFT 455 (Carl Zeiss, Germany) as well as a BP480/40 emission filter (Carl Zeiss, Germany) was used for donor excitation and donor imaging (I_{DD}); a cube comprising a BP500/20 excitation filter (Carl Zeiss, Germany) and a dichroic mirror of DFT 515 (Carl Zeiss, Germany) as well as a BP535/30 emission filter (Carl Zeiss, Germany) was used for acceptor excitation and acceptor imaging (I_{AA}); a cube comprising a BP436/20 excitation filter (Carl Zeiss, Germany) and a dichroic mirror of DFT 455 (Carl Zeiss, Germany) as well as a BP535/30 emission filter (Carl Zeiss, Germany) was used for FRET imaging (I_{DA}). Acceptor-centric FRET efficiency (E_A) was measured according to the 3^3-FRET method as described previously [31], and donor-centric FRET efficiency (E_D) and concentration ratio (R_C) were measured according to the *E*-FRET method as described previously [32,33].

2.5. FLIP measurement

FLIP experiments were performed on a confocal microscope (Zeiss LSM 880, Germany) as described previously [26]. In short, cells were imaged prior to bleaching. Then a single region (diameter of 4 μm for CFP-FLIP, or 2.5 μm for YFP-FLIP) within the nucleus was repeatedly bleached with ten iterations of a 458 nm or 514 nm laser line (100% output). Two images were collected after each bleach pulse, with 30 s between pulses. After 19 cycles of bleaching for CFP-FLIP, or 16 cycles of bleaching for YFP-FLIP, separate measurements on the mitochondria were taken to analyze loss in fluorescence. Unbleached cells neighboring analyzed cells served as controls for photobleaching during image acquisition of each measurement. Fluorescence intensities were normalized by setting the pre-bleach fluorescence to 100% signal.

2.6. Statistics

The *p* values for data sets were analyzed by unpaired Student's *t*-test. Statistical and graphic analyses were done using the software SPSS 22.0 (SPSS, Chicago) and Origin 8.0 (OriginLab Corporation).

3. Results

3.1. BAK auto-oligomerizes on mitochondria without apoptotic stimulus

To inspect the location of BAK, cells were transfected with YFP-BAK in the presence of *Z*-VAD-FMK. 10 h after transfection, cells were immunostained for Tom20 and subsequently were imaged by using a confocal microscope (Zeiss LSM880 airyscan). In contrast to the even distribution of cells expressing YFP, the cells expressing YFP-BAK exhibited punctate distribution and co-localization of BAK with Tom20 protein (Fig. 1A), indicating that BAK localized to mitochondria. The average Coefficient of Variation (CV) value of YFP from at least 15 cells expressing YFP-BAK was about 120%, much higher than the 40% for the cells expressing YFP (Fig. 1B), further demonstrating the punctate distribution of BAK.

To confirm whether BAK auto-oligomerized and formed clusters in Hela cells [34,35], we performed quantitative *E*-FRET measurements in living cells co-expressing CFP-BAK and YFP-BAK, or CFP and YFP-BAK as the control in the presence of *Z*-VAD-FMK. Fig. 1C and D show the fluorescence images of representative cells and the corresponding apparent E_D and R_C images. Statistical E_D value from at least 20 cells co-expressing CFP-BAK and YFP-BAK was 0.221 ± 0.039, much higher than the 0.032 ± 0.041 for the control cells co-expressing CFP and YFP-BAK (Fig. 1E), suggesting that BAK oligomerized and coalesced into clusters.

3.2. BCL-XL prevents BAK oligomerization and BAK-mediated cell death

To assess the function of BCL-XL and BAK, cells were transfected with YFP-BAK, or co-transfected with CFP-BCL-XL and YFP-BAK. Cells were stained with DiIC1(5) and Hoechst before confocal imaging. In contrast to the cells expressing YFP, cells expressing BAK exhibited negative DiIC1(5) and positive pyknosis, along with apoptotic body formation, which were markedly inhibited by the co-expression of BCL-XL (Fig. 2A). Statistical results showed that co-expression of BCL-XL distinctly reduced the fraction of negative DiIC1(5) and apoptosis cells caused by the expression of BAK alone from approximately 75% to 5% (Fig. 2B), verifying the notion that BCL-XL inhibits the pro-apoptotic function of BAK.

To survey whether BCL-XL transforms the location of BAK from mitochondria into cytosol [27], cells were co-transfected with either CFP and YFP-BAK, or CFP-BCL-XL and YFP-BAK in the presence of *Z*-VAD-FMK. After immunostaining for Tom20, the cells were subsequently imaged. Cells co-expressing CFP and YFP-BAK exhibited distinct punctate BAK distribution on mitochondria, whereas the cells co-

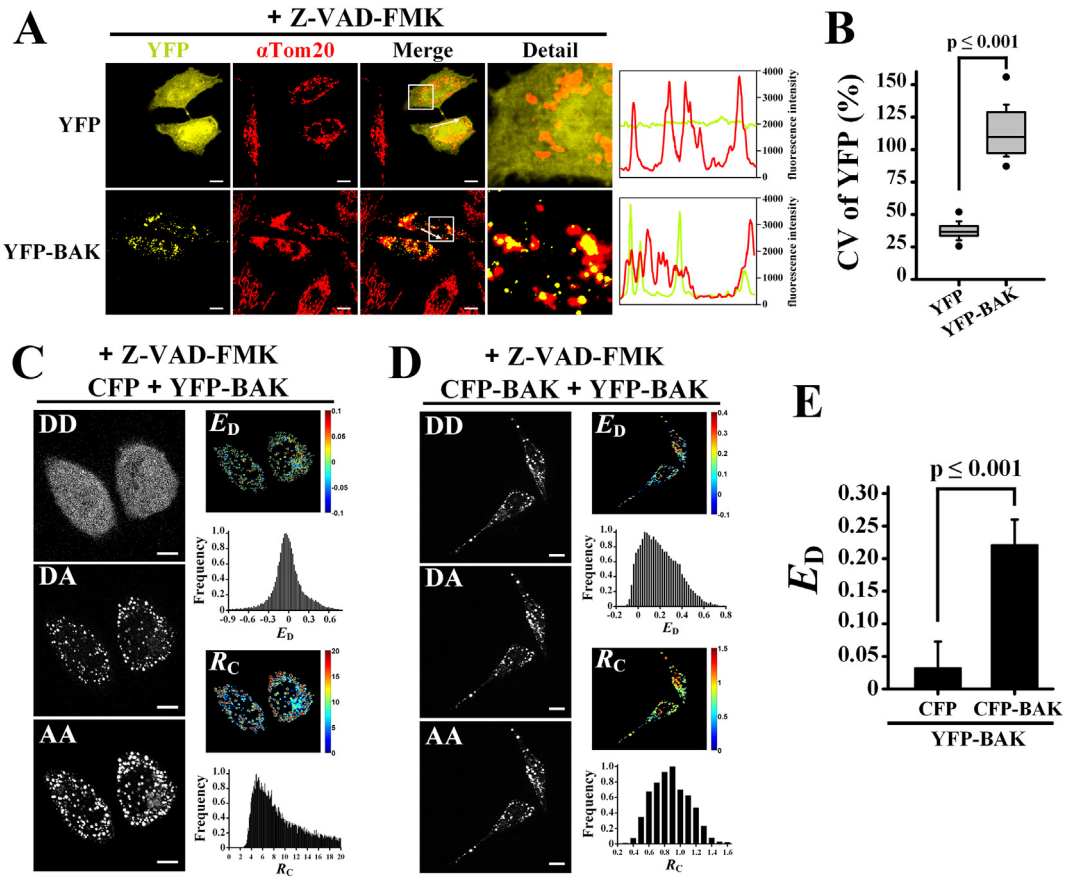

Fig. 1. BAK atuo-oligomerizes on mitochondria without apoptotic stimulus. (A) Fluorescence images of cells expressing YFP or YFP-BAK in the presence of *Z*-VAD-FMK after immunostaining for Tom20 (red). Line scans show the fluorescence intensities of YFP-signals (yellow) and mitochondria stained by α-Tom20 staining (red) along the selected white arrow line in the merge panel. Scale bar: 10 μm. (B) Coefficient of Variation (CV) values of the YFP fluorescence of cells expressing YFP or YFP-BAK in the presence of *Z*-VAD-FMK. Dots represent the extreme data points of CV. $n \geq 15$ cells. (C) Three fluorescence images in DD, DA and AA channels (left) of the living cells co-expressing CFP and YFP-BAK in the presence of *Z*-VAD-FMK, and the corresponding pixel-to-pixel E_D and R_C images and histograms (right). Scale bar: 10 μm. (D) Similar images to (C) of the living cells co-expressing CFP-BAK and YFP-BAK in the presence of Z-VAD-FMK. (E) Statistical E_D values of living cells co-expressing CFP and YFP-BAK, or CFP-BAK and YFP-BAK. Data represent averages ± SD. $n \geq 20$ cells. (For interpretation of the references to colour in this figure legend, the reader is referred to the web version of this article.)

expressing CFP-BCL-XL and YFP-BAK exhibited partly cytoplasmic distribution of BAK (Fig. 2C), demonstrating that BCL-XL prevented mitochondrial location of BAK. The average CV value of YFP-BAK from at least 15 cells decreased from 120% for the cells co-expressing CFP and YFP-BAK to 47% for the cells co-expressing CFP-BCL-XL and YFP-BAK (Fig. 2D), further demonstrating the notion that BCL-XL prevents the mitochondrial punctate location of BAK.

To explore whether BCL-XL prevents BAK oligomerization, we performed quantitative *E*-FRET measurements in living cells co-expressing CFP-BAK and YFP-BAK in the absence (Fig. 1D) or presence (Fig. 2E) of UT-BCL-XL (no fluorescent label). Fig. 2E shows the representative quantitative E-FRET measurements for the cells co-expressing CFP-BAK and YFP-BAK in the presence of UT-BCL-XL. Statistical E_D value from at least 20 cells co-expressing CFP-BAK and YFP-BAK in the presence of UT-BCL-XL was 0.034 ± 0.023, much lower than the 0.221 ± 0.039 for the cells in the absence of UT-BCL-XL (Fig. 2F), indicating that BCL-XL prevented BAK oligomerization. In addition, FRET analysis showed that the E_D value (0.034 ± 0.023) of cells co-expressing CFP-BAK and YFP-BAK in the presence of UT-BCL-XL was similar to that (0.032 ± 0.041) of the control cells co-expressing CFP and YFP-BAK (Fig. 2E and F), demonstrating that there were almost no BAK dimers or oligomers in the cells with excessive BCL-XL [23,36].

In order to further verify that the high E_D value of BAK clusters was not caused by the random collisions between mitochondrial BAK monomers, we measured the E_D value between cytosolic and mitochondrial CFP-BAK and YFP-BAK in the presence of UT-BCL-XL. As shown in Fig. S1, although the E_D value (0.109 ± 0.031) between clumped-mitochondrial CFP-BAK and YFP-BAK was modestly higher than that (0.060 ± 0.045) between cytosolic CFP-BAK and YFP-BAK, it was much lower than the E_D value (0.221 ± 0.039) between CFP-BAK and YFP-BAK in the absence UT-BCL-XL (Fig. 1D), further verifying that the random collisions between clumped-mitochondrial BAK monomers had not been falsely interpreted as BAK oligomerization.

3.3. BCL-XL physically restrains and retrotranslocates monomeric BAK

To investigate whether BCL-XL directly sequestrates monomeric BAK [25,37], we performed quantitative *E*-FRET measurements in living cells co-expressing CFP-BCL-XL and YFP-BAK. Fig. 3A and B show the fluorescence images of representative cells and the corresponding apparent E_A and R_C images. Statistical E_A value from at least 30 cells co-expressing CFP-BCL-XL and YFP-BAK was 0.226 ± 0.032, much higher than the 0.112 ± 0.033 for the control cells co-expressing CFP-BCL-XL and YFP (Fig. 3C), evidencing that BCL-XL associated with monomeric BAK to form hetero-oligomers for preventing BAK oligomerization.

To confirm BCL-XL retrotranslocated monomeric BAK and thus resulted in partial cytosolic BAK location, we performed FLIP experiments in living cells expressing YFP-BAK in the absence or presence of CFP-BCL-XL on the confocal microscope. We used a 514 nm laser line to repeatedly bleach a nuclear region (Fig. 3D, red square) and

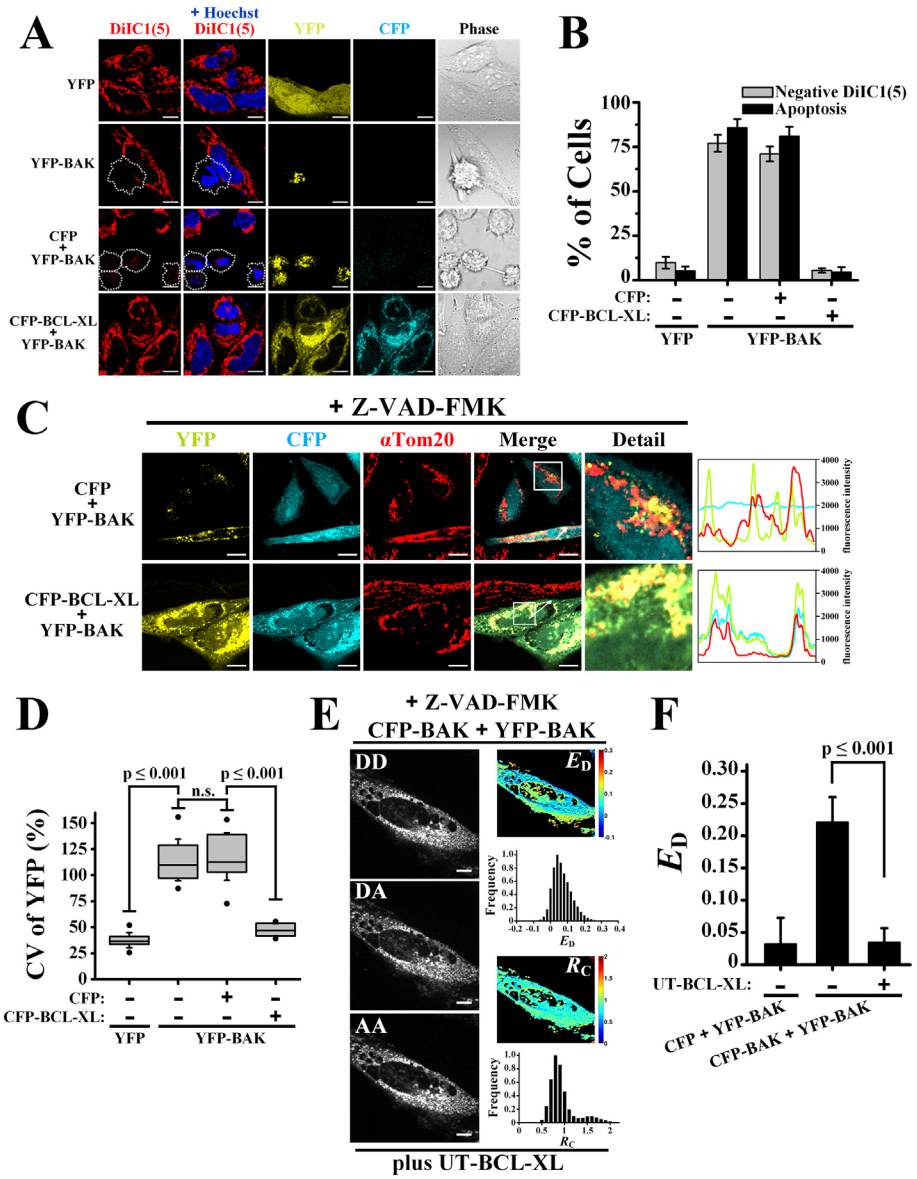

Fig. 2. BCL-XL prevents BAK oligomerization and BAK-mediated cell death. (A) Fluorescence images of cells expressing YFP or YFP-BAK, or co-expressing CFP and YFP-BAK, or CFP-BCL-XL and YFP-BAK after staining with DiIC1(5) (red) and Hoechst (blue). The broken spline contours show the DiIC1(5)-negative cells. Scale bar: 10 μm. (B) Statistical percentages of negative DiIC1(5) and apoptosis cells. Data represent averages of triplicates ± SD; $n \geq 150$ cells. (C) Fluorescence images of cells co-expressing CFP and YFP-BAK, or CFP-BCL-XL and YFP-BAK in the presence of *Z*-VAD-FMK after immunostaining for Tom20 (red). Line scans show the fluorescence intensities of YFP-signals (yellow), CFP-signals (cyan) and mitochondria stained by α-Tom20 staining (red) along the selected white arrow line in the merge panel. Scale bar: 10 μm. (D) CV values of the YFP fluorescence of cells expressing YFP or YFP-BAK (data from Fig. 1B), or co-expressing CFP and YFP-BAK, or CFP-BCL-XL and YFP-BAK, in the presence of Z-VAD-FMK. Dots represent the extreme data points of CV. n ≥ 15 cells. n.s. = no statistical significance. (E) Three fluorescence images in DD, DA and AA channels (left) of the living cells co-expressing CFP-BAK and YFP-BAK in the presence of UT-BCL-XL (no fluorescent label) and Z-VAD-FMK, and the corresponding the pixel-to-pixel E_D and R_C images and histograms (right). Scale bar: 10 μm. (F) Statistical E_D values of living cells co-expressing CFP and YFP-BAK in the absence of UT-BCL-XL (data from Fig. 1E), or CFP-BAK and YFP-BAK in the absence (data from Fig. 1E) or presence of UT-BCL-XL. Data represent averages ± SD. $n \geq 20$ cells. (For interpretation of the references to colour in this figure legend, the reader is referred to the web version of this article.)

subsequently imaged CFP and YFP after per bleach. A ROI measurement in the neighboring cell was chose as a control for cell-specific bleaching (Fig. 3D, purple cycle). As shown in Fig. 3D, YFP-fluorescence on mitochondria of the cells expressing YFP-BAK alone was not weakened during the FLIP experiments, whereas YFP-fluorescence on mitochondria of the cells in the presence of CFP-BCL-XL gradually diminished by repeated bleaching, indicating monomeric BAK shuttling between mitochondria and cytosol by BCL-XL. We fitted FLIP curves of the dynamical mitochondrial YFP-fluorescence intensity from 15 ROI measurements by one Exponential Decay model (Fig. 3E), and found that the retrotranslocation rate of monomeric BAK in the absence of CFP-BCL-XL was $0.023 \pm 5.456 \times 10^{-3} S^{-1}$, much slower than the $7.872 \pm 5.018 \times 10^{-3} S^{-1}$ in the presence of CFP-BCL-XL (Fig. 3F), demonstrating that BCL-XL increased the retrotranslocation rate of monomeric BAK.

3.4. Monomeric BAK reduces the retrotranslocation rate of BCL-XL

Based on the finding that BAX increased BCL-XL shuttling from mitochondria into cytosol [26,38], we were thus curious about whether BAK also increased the retrotranslocation rate of BCL-XL. FLIP experiments in living cells co-expressing CFP-BCL-XL and YFP, or CFP-BCL-XL and YFP-BAK, were performed on the confocal microscope with 458 nm laser excitation just as described in Fig. 3D. As shown in Fig. 4A, mitochondrial CFP-fluorescence of the cells co-expressing CFP-BCL-XL and YFP weakened faster than that of the cells co-expressing CFP-BCL-XL and YFP-BAK by repeated bleaching with 458 nm laser excitation. We depicted the decay of mitochondrial CFP-BCL-XL fluorescence intensity from 24 ROI measurements by one Exponential Decay model (Fig. 4B), and found that the retrotranslocation rate of BCL-XL for cells co-expressing CFP-BCL-XL and YFP was $6.158 \pm 2.120 \times 10^{-3} S^{-1}$, faster than the $4.585 \pm 1.534 \times 10^{-3} S^{-1}$ for cells co-expressing CFP-BCL-XL and YFP-BAK (Fig. 4C), demonstrating that monomeric BAK reduced the retrotranslocation rate of BCL-XL.

3.5. BCL-XL does not depolymerize and retrotranslocate the oligomerized BAK

Based on the fact that BCL-XL potently prevented mitochondrial BAK oligomerization (Fig. 2E and F), we wonder whether BCL-XL depolymerized the oligomerized BAK. To answer this issue, cells were first transfected with YFP-BAK for 14 h in the presence of *Z*-VAD-FMK for inducing BAK auto-oligomerization, and subsequently were transfected with CFP-BCL-XL for 12 h (Fig. 5A). After staining with DiIC1(5),

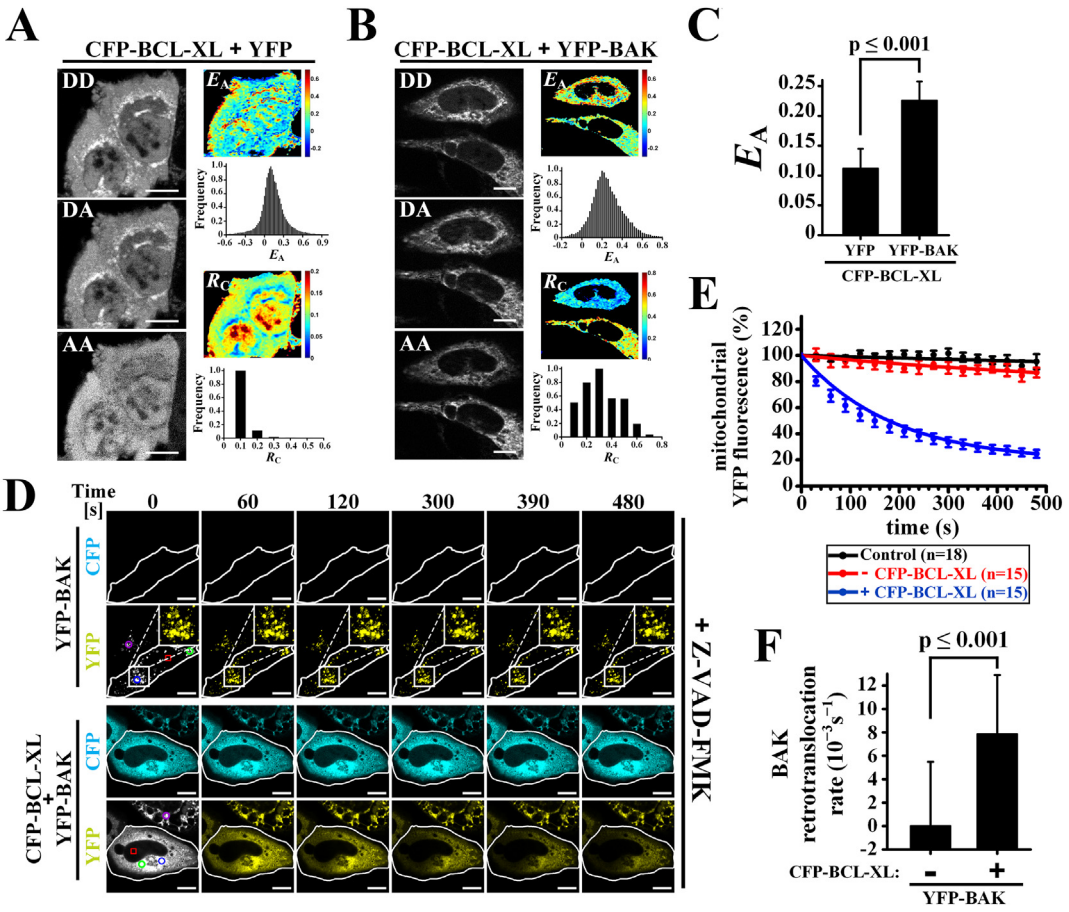

Fig. 3. BCL-XL physically restrains and retrotranslocates monomeric BAK. (A) Three fluorescence images in DD, DA and AA channels (left) of living cells co-expressing CFP-BCL-XL and YFP, and the corresponding the pixel-to-pixel E_A and R_C images and histograms (right). Scale bar: 10 μm. (B) Similar images to (A) of the living cells co-expressing CFP-BCL-XL and YFP-BAK. (C) Statistical E_A values of living cells co-expressing CFP-BCL-XL and YFP, or CFP-BCL-XL and YFP-BAK. Data represent averages ± SD. $n \geq 30$ cells. (D) Fluorescence loss in photobleaching (FLIP) analysis of YFP-BAK in the absence or presence of CFP-BCL-XL, in the presence of *Z*-VAD-FMK. The regions (red square) are bleached at 514 nm in the both targeted cells (white spline contours). Changes in BAK fluorescence on the mitochondria are detected in marked areas (green and blue circle, respectively), whereas a ROI measurement in the neighboring cell serves as a control for cell-specific bleaching (purple circle). The detail images within the second panels are the enlarged views of the white squares. Time points in seconds are displayed above the pictures. Scale bar: 10 μm. (E) FLIP curves of the dynamical mitochondrial YFP-BAK in the absence (red) or presence (blue) of CFP-BCL-XL by one Exponential Decay model. Fluorescence of the neighboring cell is shown as control (black). Data represent averages ± SEM. n = number of ROI measurements per condition. (F) Retrotranslocation rates measured for BAK in the absence or presence of CFP-BCL-XL. Data represent averages ± SD. (For interpretation of the references to colour in this figure legend, the reader is referred to the web version of this article.)

confocal imaging showed that the cells expressing BAK exhibited BAK oligomerization and negative DiIC1(5), which were obviously inhibited by the post-transfection with BCL-XL (Fig. 5B). Statistical results showed that post-transfection of BCL-XL distinctly reduced the fraction of cells with BAK oligomerization and negative DiIC1(5) caused by expression of BAK alone from approximately 80% to 30% (Fig. 5C), implicating the possibility that BCL-XL depolymerized the oligomerized BAK.

We next performed live-cell fluorescence imaging to assess the depolymerization and retrotranslocation of the oligomerized BAK by BCL-XL in the living cells that were firstly transfected with YFP-BAK for 14 h and subsequently transfected with CFP-BCL-XL. As shown in Fig. 5D, in the presence of CFP-BCL-XL, the cells with BAK clusters still exhibited punctate BAK distribution during observation. Moreover, the CV values of the YFP fluorescence of the cell were still higher than 130% (Fig. 5D), demonstrating that BCL-XL did not depolymerize the oligomerized BAK. In addition, the cell expressing CFP-BCL-XL before BAK oligomerization always exhibited even BAK distribution, and the corresponding CV values of the YFP fluorescence were still lower than 21% during observation (Fig. 5E), indicating that BCL-XL did prevent the formation of BAK oligomers. To confirm whether BCL-XL retrotranslocates the oligomerized BAK, FLIP experiments in living cells were performed on the confocal microscope with 514 nm laser excitation just as described in Fig. 3D. YFP-BAK clusters were not weakened by repeated bleaching of cytosol YFP-BAK (Fig. 5F). We fitted FLIP curves of the dynamical YFP-fluorescence intensity in both the cytosol and BAK clusters from 10 ROI measurements by one Exponential Decay model. The YFP fluorescence of the BAK clusters weakened similar to the control and much slower than that of the cytosol region (Fig. 5F), further verifying that BCL-XL did not retrotranslocate the oligomerized BAK.

4. Discussion

Our data firmly demonstrate that BCL-XL prevents the oligomerization and pro-apoptotic ability of BAK by inhibiting the formation of BAK oligomers and retrotranslocating the monomeric BAK from mitochondria into cytosol. In vitro evidences have certified the notion that BCL-XL physically sequestrates monomeric BAK to inhibit the pro-apoptotic function of BAK [22,37]. We here used live-cell imaging techniques including FRET and FLIP to assess the regulation way of BCL-XL on BAK shuttling between mitochondria and cytosol [27]. Live-cell imaging and FRET experiments verify that BCL-XL directly

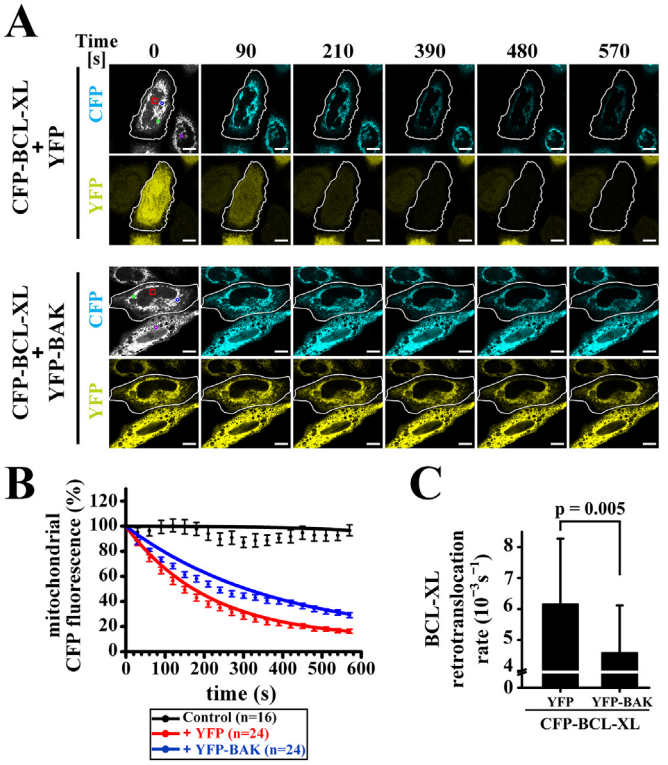

Fig. 4. Monomeric BAK reduces the retrotranslocation rate of BCL-XL. (A) FLIP analysis of CFP-BCL-XL in the absence or presence of YFP-BAK. The regions (red square) are bleached at 458 nm in the both targeted cells (white spline contours). Changes in BCL-XL fluorescence on mitochondria are detected in marked areas (green and blue circle, respectively), whereas a ROI measurement in the neighboring cell serves as a control for cell-specific bleaching (purple circle). Time points in seconds are displayed above the pictures. Scale bar: 10 μm. (B) FLIP curves of the dynamical mitochondrial CFP-BCL-XL in the absence (red) or presence (blue) of YFP-BAK by one Exponential Decay model. Fluorescence of the neighboring cell is shown as control (black). Data represent averages ± SEM. n = number of ROI measurements per condition. (C) Retrotranslocation rates measured for BCL-XL in the absence or presence of YFP-BAK. Data represent averages ± SD. (For interpretation of the references to colour in this figure legend, the reader is referred to the web version of this article.)

sequestrates the monomeric BAK to prevent BAK oligomerization and BAK-mediated cell death. FLIP analyses indicate that BCL-XL increases the monomeric BAK shuttling from mitochondria into cytosol, whereas monomeric BAK reduces the retrotranslocation rate of BCL-XL. Moreover, live-cell time-lapse imaging and FLIP experiments demonstrate that BCL-XL does not depolymerize and retrotranslocate the oligomerized BAK.

Whether BAK auto-oligomerizes on mitochondria without apoptotic stimulus remains controversial. BN-PAGE and SDS-PAGE analyses on the isolated mitochondria from WT or $BAX^{-/-}BAK^{-/-}$ (DKO) MEFs incubated with BAK showed that BAK always maintained its inactive structure on mitochondria in the absence of apoptotic stimulus [39,40], indicating that BAK did not auto-oligomerize on mitochondria without apoptotic stimulation. Furthermore, living Cos-7, Hela and HCT116 DKO cells expressing FP-BAK did not show BAK clusters, but showed good co-localization of BAK with mitochondria [27,34,35], further indicating that BAK did not auto-oligomerize without apoptotic stimulus. These aforementioned studies support the idea that although being predominantly mitochondrial, BAK leads to apoptosis only in the presence of apoptotic stimuli [27,41]. However, incubation with BAK on the isolated mitochondria from Hela cells without apoptotic stimulus showed oligomerized BAK, indicating that BAK auto-oligomerized on mitochondria [40]. Moreover, expression of BAK markedly induced cyt c release and apoptosis in Hela cells without apoptotic stimulus [42], which may be due to the BAK auto-oligomerization. Our FRET analysis on the cells co-expressing CFP-BAK and YFP-BAK showed much higher E_D value (> 20%) than that of the control cells, indicating that BAK oligomerized and coalesced into clusters without apoptotic stimulus (Fig. 1C–E). Furthermore, the cells with BAK clusters exhibited negative DiIC1(5) (mitochondrial depolarization) (Fig. 5B and C), whereas the cells without BAK clusters exhibited positive DiIC1(5) (mitochondrial polarization) (Fig. S2), demonstrating that the oligomerized BAK permeabilizes MOM [43], and thus the BAK clusters are definitely active BAK oligomers in our conditions.

In contrast to the increasing retrotranslocation of monomeric BAK by BCL-XL (Fig. 3D–F), monomeric BAK reduced the retrotranslocation rate of BCL-XL (Fig. 4). It was reported that BAK bound to BCL-XL to co-retrotranslocate from mitochondria into cytosol [27]. FRET analysis on the cells co-expressing CFP-BCL-XL and YFP-BAK showed much higher E_A value (> 20%) than that of control cells (Fig. 3A–C), supporting the notion that BAK physically binds to BCL-XL to form hetero-oligomers. BCL-XL natively shuttles between mitochondria and cytosol, whereas BAK stably anchors in MOM (Figs. 3 and 4) [26,27,38]. It is the high-affinity of BAK with MOM [27] that decreases the retrotranslocation rate of BCL-XL/BAK hetero-oligomers (Fig. 3A-C). Therefore, BCL-XL increases the retrotranslocation of monomeric BAK, while monomeric BAK decreases the retrotranslocation of BCL-XL, which further verifies the notion that monomeric BAK is co-retrotranslocated with BCL-XL in hetero-oligomer form [27].

Besides the BCL-XL bound to BAK, there are different BCL-XL forms, such as monomeric BCL-XL, BCL-XL bound to BCL-XL, BCL-XL bound to BAX, and BCL-XL bound to BH3-only proteins [26,44,45]. Our recent FRET two-hybrid analyses in living cells co-expressing CFP-BCL-XL and YFP-BCL-XL, or CFP-BAX and YFP-BCL-XL, or CFP-BCL-XL and BAD-YFP, or CFP-BCL-XL and YFP-tBID, exhibiting larger than 20% of FRET efficiency (E_D or E_A) (data not shown), support that BCL-XL can bind to BCL-XL, BAX, BAD and tBID, respectively.

The model of BCL-XL dimerization [46] can be used to explain why BCL-XL retrotranslocates natively and retrotranslocates monomeric BAK/BAX from mitochondria into cytosol. The hydrophobic C-terminal tail of BCL-XL is shield in dimer through the direct bindings of C-terminal tail of one to the hydrophobic groove of the other one [44,46]. Consequently, BCL-XL is thought to spontaneously retrotranslocate from mitochondria to cytoplasm in homo-dimer. In this scenario, monomeric BAK/BAX binds to BCL-XL to dissociate the BCL-XL dimers and form hetero-oligomers. The hydrophobic C-terminal tails of both BCL-XL and monomeric BAK/BAX are shield in the oligomer through the direct bindings of C-terminal tail of one to the hydrophobic groove of the other one, thus triggering the retrotranslocation of the hetero-oligomers. Although BH3-only proteins can also bind to BCL-XL to form hetero-oligomers [45], BH3-only proteins lack the hydrophobic groove to shield the hydrophobic C-terminal tail of BCL-XL [47]. Therefore, contrast to increasing the retrotranslocation of monomeric BAK/BAX by BCL-XL, BCL-XL may decrease the retrotranslcation of BH3-only proteins [45,48].

Our data support the notion that BCL-XL does not depolymerize and retrotranslocate the oligomerized BAK (Fig. 5D and F). Based on the findings that BAK oligomerization is a reversible process [28] and BCL-XL potently inhibits the pro-apoptotic function of BAK (Fig. 2), we initially conjectured that BCL-XL may depolymerize the oligomerized BAK to inhibit the pro-apoptotic function of BAK. To explore this issue, cells were first transfected with YFP-BAK to obtain cells with auto-oligomerized BAK, and subsequently were transfected with CFP-BCL-XL (Fig. 5A). About 70% cells co-expressing BAK and BCL-XL did not exhibit punctate BAK distribution, while most of the cells expressing BAK alone exhibited punctate BAK distribution (Fig. 5B and C). We thus inferred that BCL-XL depolymerized the oligomerized BAK. To further verify this issue, we performed live-cell time-lapse imaging and FLIP experiments for the cells with BAK clusters in the presence of BCL-XL.

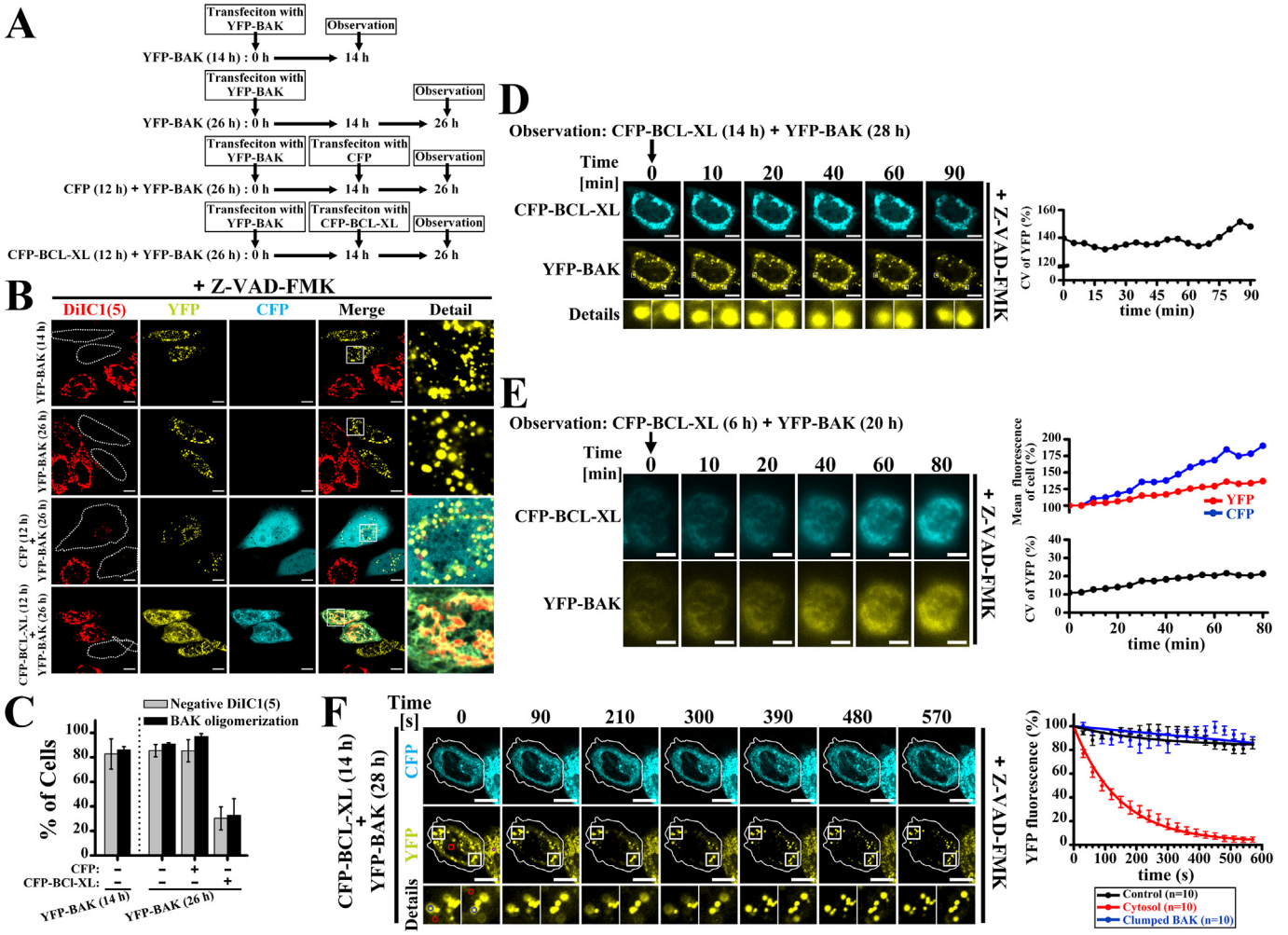

Fig. 5. BCL-XL does not depolymerize and retrotranslocate the oligomerized BAK. (A) Time flow of fluorescence imaging experiments. Cells transfected with YFP-BAK alone for 14 h and subsequently transfected with CFP-BCL-XL for 12 h in the presence of *Z*-VAD-FMK. (B) Fluorescence images of cells transfected with YFP-BAK alone for 14 h and subsequently transfected with CFP-BCL-XL for 12 h after staining with DiIC1(5) (red). The broken spline contours show the DiIC1(5)-negative cells. Scale bar: 10 μm. (C) Statistical percentages of cells with negative DiIC1(5) and oligomerized BAK. Data represent averages of triplicates ± SD; $n \geq 120$ cells. (D) Time-lapse imaging of a representative cell that was firstly transfected with YFP-BAK for 14 h and subsequently transfected with CFP-BCL-XL for 14 h in the presence of Z-VAD-FMK. The details images in the low panel are the enlarged views of BAK clusters in marked areas (white squares) in the middle panel. Time stamps indicate time during observation. Line plot shows the dynamical CV values of the YFP fluorescence of the cell. Scale bar: 10 μm. (E) Time-lapse imaging of a representative cell that was firstly transfected with YFP-BAK for 14 h and subsequently transfected with CFP-BCL-XL for 6 h in the presence of Z-VAD-FMK. Time stamps indicate time during observation. Line plots show the changes in CFP (blue) and YFP (red) fluorescence of the cell, and the dynamical CV values (black) of YFP fluorescence of the cell. Scale bar: 10 μm. (F) BCL-XL does not retrotranslocate the oligomerized BAK. The targeted cell (white spline contour), exhibiting BAK clusters in the presence of CFP-BCL-XL, is bleached in FLIP experiments in the region marked as red square with 514 nm excitation. The details images in the low panel are the enlarged views of the marked areas (white squares) in the middle panel. Changes in YFP fluorescence of the cytosol (red circle) and BAK clusters (blue circle) are detected respectively, whereas a ROI measurement in the neighboring cell serves as a control for cell-specific bleaching (purple circle). Time points in seconds are displayed above the pictures. FLIP curves of the dynamical YFP fluorescence of cytosol (red) and BAK clusters (blue) were fitted by one Exponential Decay model. Fluorescence of the neighboring cell is shown as control (black). Data represent averages ± SEM. n = number of ROI measurements per condition. Scale bar: 10 μm. (For interpretation of the references to colour in this figure legend, the reader is referred to the web version of this article.)

To our great disappointment, we found that BCL-XL did not depolymerize and retrotranslocate the oligomerized BAK (Fig. 5D and F). Although we had no direct evidence about the binding of BCL-XL to the BAK monomer, FRET analysis (Figs. 3A–C and 2E,F and S1) demonstrated that BCL-XL physically bound to monomeric BAK to form hetero-oligomers and there were almost no BAK dimers or oligomers in the cells with excessive BCL-XL [23,36]. Furthermore, we also found that BCL-XL did prevent the formation of BAK oligomers (Fig. 5E). Therefore, we conclude that BCL-XL directly interacts with BAK monomer to co-retrotranslocate from mitochondria into cytosol.

The oligomerized BAK may not possess binding site with BCL-XL. It is generally known that BCL-XL sequestrates monomeric BAK by the binding of the hydrophobic groove of BCL-XL with the BH3 domain of BAK [43], which is also further verified by the evidences that the BAK BH3 domain mutant (e.g. BAK^{Q75L}, BAK^{R76A} and BAK^{Q77A}) does not interact with BCL-XL [25]. During BAK oligomerization, BAK exposes its BH3 domain to interact with the groove of another BAK to form symmetric dimers without exposed BH3 domain [4,5,49,50]. In addition, BN-PAGE and SDS-PAGE analyses on the isolated mitochondria incubated with BAK dimers and BCL-XL showed that BCL-XL did not interfere with the linkage between BAK dimers [28], indicating that BCL-XL did not disrupt the interdimer interactions of α6/α6 or α3/α5 [51,52] in BAK oligomers, even though the interdimer interactions are weaker than the intradimer ones [28,53].

In summary, we provide ex vivo evidence that BCL-XL physically sequestrates the monomeric BAK to inhibit the pro-apoptotic function

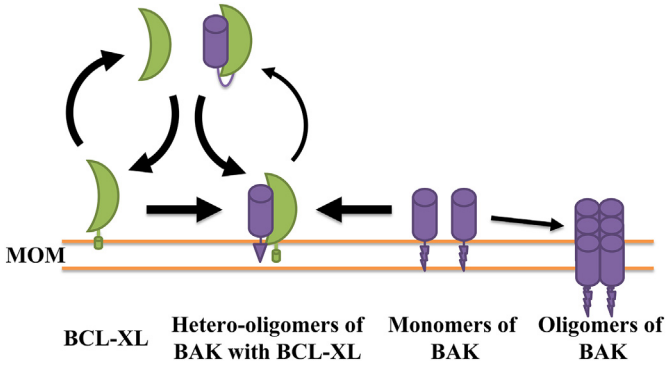

Fig. 6. Schematic model showing the regulation of BCL-XL on retro-translocating BAK.

of BAK, and summarize the regulation mechanism of BCL-XL on BAK in Fig. 6. We highlight BCL-XL does not depolymerize and retrotranslocate the oligomerized BAK. BCL-XL shuttles between mitochondria and cytosol spontaneously, and directly binds to the monomeric BAK to co-retrotranslocate from mitochondria into cytosol, thus inhibiting BAK oligomerization.

Funding

This work was supported by the National Natural Science Foundation of China (grant numbers: 61527825, 61875056 and 81572184).

Conflict of interest statement

The authors have declared that no competing interests exist.

Acknowledgments

We would like to thank Prof. A.P. Gilmore for providing CFP-BCL-XL plasmid.

Appendix A. Supplementary data

Supplementary data to this article can be found online at https://doi.org/10.1016/j.cellsig.2019.05.001.

References

[1] T. Lindsten, A.J. Ross, A. King, W.X. Zong, J.C. Rathmell, H.A. Shiels, E. Ulrich, K.G. Waymire, P. Mahar, K. Frauwirth, Y. Chen, M. Wei, V.M. Eng, D.M. Adelman, M.C. Simon, A. Ma, J.A. Golden, G. Evan, S.J. Korsmeyer, G.R. MacGregor, C.B. Thompson, The combined functions of proapoptotic Bcl-2 family members Bak and Bax are essential for normal development of multiple tissues, Mol. Cell 6 (2000) 1389–1399, https://doi.org/10.1016/s1097-2765(00)00136-2.

[2] M.C. Wei, W.X. Zong, E.H. Cheng, T. Lindsten, V. Panoutsakopoulou, A.J. Ross, K.A. Roth, G.R. MacGregor, C.B. Thompson, S.J. Korsmeyer, Proapoptotic Bax and Bak: a requisite gateway to mitochondrial dysfunction and death, Science 292 (2001) 727–730, https://doi.org/10.1126/science.1059108.

[3] S. Bleicken, O. Landeta, A. Landajuela, G. Basanez, A.J. Garcia-Saez, Proapoptotic Bax and Bak proteins form stable protein-permeable pores of tunable size, J. Biol. Chem. 288 (2013) 33241–33252, https://doi.org/10.1074/jbc.M113.512087.

[4] J.M. Brouwer, D. Westphal, G. Dewson, A.Y. Robin, R.T. Uren, R. Bartolo, G.V. Thompson, P.M. Colman, R.M. Kluck, P.E. Czabotar, Bak core and latch domains separate during activation, and freed core domains form symmetric homodimers, Mol. Cell 55 (2014) 938–946, https://doi.org/10.1016/j.molcel.2014.07.016.

[5] A.E. Alsop, S.C. Fennell, R.C. Bartolo, I.K. Tan, G. Dewson, R.M. Kluck, Dissociation of Bak Alpha1 Helix from the core and latch domains is required for apoptosis, Nat. Commun. 6 (2015) 6841, , https://doi.org/10.1038/ncomms7841.

[6] S.B. Bratton, G.M. Cohen, Caspase cascades in chemically-induced apoptosis, Adv. Exp. Med. Biol. 500 (2001) 407–420, https://doi.org/10.1007/978-1-4615-0667-6_63.

[7] D.R. Green, G. Kroemer, The pathophysiology of mitochondrial cell death, Science 305 (2004) 626–629, https://doi.org/10.1126/science.1099320.

[8] Y. Liang, M.A. Eid, R.W. Lewis, M.V. Kumar, Mitochondria from trail-resistant prostate cancer cells are capable of responding to apoptotic stimuli, Cell. Signal. 17 (2005) 243–251, https://doi.org/10.1016/j.cellsig.2004.07.006.

[9] L.J. Hsu, Q. Hong, L. Schultz, E. Kuo, S.R. Lin, M.H. Lee, Y.S. Lin, N.S. Chang, Zfra is an inhibitor of Bcl-2 expression and cytochrome C release from the mitochondria, Cell. Signal. 20 (2008) 1303–1312, https://doi.org/10.1016/j.cellsig.2008.02.018.

[10] H. Kim, H.C. Tu, D. Ren, O. Takeuchi, J.R. Jeffers, G.P. Zambetti, J.J. Hsieh, E.H. Cheng, Stepwise activation of Bax and Bak by Tbid, Bim, and Puma initiates mitochondrial apoptosis, Mol. Cell 36 (2009) 487–499, https://doi.org/10.1016/j.molcel.2009.09.030.

[11] P.F. Cartron, E. Petit, G. Bellot, L. Oliver, F.M. Vallette, Metaxins 1 and 2, two proteins of the mitochondrial protein sorting and assembly machinery, are essential for Bak activation during Tnf alpha triggered apoptosis, Cell. Signal. 26 (2014) 1928–1934, https://doi.org/10.1016/j.cellsig.2014.04.021.

[12] H. Dussmann, M. Rehm, C.G. Concannon, S. Anguissola, M. Wurstle, S. Kacmar, P. Voller, H.J. Huber, J.H. Prehn, Single-cell quantification of Bax activation and mathematical modelling suggest pore formation on minimal mitochondrial Bax accumulation, Cell Death Differ. 17 (2010) 278–290, https://doi.org/10.1038/cdd.2009.123.

[13] S.B. Ma, T.N. Nguyen, I. Tan, R. Ninnis, S. Iyer, D.A. Stroud, M. Menard, R.M. Kluck, M.T. Ryan, G. Dewson, Bax targets mitochondria by distinct mechanisms before or during apoptotic cell death: a requirement for Vdac2 or Bak for efficient Bax apoptotic function, Cell Death Differ. 21 (2014) 1925–1935, https://doi.org/10.1038/cdd.2014.119.

[14] E. Petit, P.F. Cartron, L. Oliver, F.M. Vallette, The phosphorylation of metaxin 1 controls Bak activation during Tnfalpha induced cell death, Cell. Signal. 30 (2017) 171–178, https://doi.org/10.1016/j.cellsig.2016.11.008.

[15] J.E. Chipuk, T. Moldoveanu, F. Llambi, M.J. Parsons, D.R. Green, The Bcl-2 family reunion, Mol. Cell 37 (2010) 299–310, https://doi.org/10.1016/j.molcel.2010.01.025.

[16] E.M. Kim, J. Kim, J.K. Park, S.G. Hwang, W.J. Kim, W.J. Lee, S.W. Kang, H.D. Um, Bcl-W promotes cell invasion by blocking the invasion-suppressing action of Bax, Cell. Signal. 24 (2012) 1163–1172, https://doi.org/10.1016/j.cellsig.2012.01.019.

[17] M. Gomez-Benito, P. Balsas, X. Carvajal-Vergara, A. Pandiella, A. Anel, I. Marzo, J. Naval, Mechanism of apoptosis induced by Ifn-alpha in human myeloma cells: role of Jak1 and Bim and potentiation by rapamycin, Cell. Signal. 19 (2007) 844–854, https://doi.org/10.1016/j.cellsig.2006.10.009.

[18] D. Ren, H.C. Tu, H. Kim, G.X. Wang, G.R. Bean, O. Takeuchi, J.R. Jeffers, G.P. Zambetti, J.J. Hsieh, E.H. Cheng, Bid, Bim, and Puma are essential for activation of the Bax- and Bak-dependent cell death program, Science 330 (2010) 1390–1393, https://doi.org/10.1126/science.1190217.

[19] W. Zhang, X. Wang, T. Chen, Resveratrol induces apoptosis via a Bak-mediated intrinsic pathway in human lung adenocarcinoma cells, Cell. Signal. 24 (2012) 1037–1046, https://doi.org/10.1016/j.cellsig.2011.12.025.

[20] F. Llambi, T. Moldoveanu, S.W. Tait, L. Bouchier-Hayes, J. Temirov, L.L. McCormick, C.P. Dillon, D.R. Green, A unified model of mammalian Bcl-2 protein family interactions at the mitochondria, Mol. Cell 44 (2011) 517–531, https://doi.org/10.1016/j.molcel.2011.10.001.

[21] P.E. Czabotar, G. Lessene, A. Strasser, J.M. Adams, Control of apoptosis by the Bcl-2 protein family: implications for physiology and therapy, Nat. Rev. Mol. Cell Biol. 15 (2014) 49–63, https://doi.org/10.1038/nrm3722.

[22] C. Hockings, A.E. Alsop, S.C. Fennell, E.F. Lee, W.D. Fairlie, G. Dewson, R.M. Kluck, Mcl-1 and Bcl-xl sequestration of Bak confers differential resistance to Bh3-only proteins, Cell Death Differ. 25 (2018) 719–732, https://doi.org/10.1038/s41418-017-0010-6.

[23] H.C. Chen, M. Kanai, A. Inoue-Yamauchi, H.C. Tu, Y. Huang, D. Ren, H. Kim, S. Takeda, D.E. Reyna, P.M. Chan, Y.T. Ganesan, C.P. Liao, E. Gavathiotis, J.J. Hsieh, E.H. Cheng, An interconnected hierarchical model of cell death regulation by the Bcl-2 family, Nat. Cell Biol. 17 (2015) 1270–1281, https://doi.org/10.1038/ncb3236.

[24] K.L. O'Neill, K. Huang, J. Zhang, Y. Chen, X. Luo, Inactivation of prosurvival Bcl-2 proteins activates Bax/Bak through the outer mitochondrial membrane, Genes Dev. 30 (2016) 973–988, https://doi.org/10.1101/gad.276725.115.

[25] E.F. Lee, S. Grabow, S. Chappaz, G. Dewson, C. Hockings, R.M. Kluck, M.A. Debrincat, D.H. Gray, M.T. Witkowski, M. Evangelista, A. Pettikiriarachchi, P. Bouillet, R.M. Lane, P.E. Czabotar, P.M. Colman, B.J. Smith, B.T. Kile, W.D. Fairlie, Physiological restraint of Bak by Bcl-xl is essential for cell survival, Genes Dev. 30 (2016) 1240–1250, https://doi.org/10.1101/gad.279414.116.

[26] F. Edlich, S. Banerjee, M. Suzuki, M.M. Cleland, D. Arnoult, C. Wang, A. Neutzner, N. Tjandra, R.J. Youle, Bcl-X(L) retrotranslocates Bax from the mitochondria into the cytosol, Cell 145 (2011) 104–116, https://doi.org/10.1016/j.cell.2011.02.034.

[27] F. Todt, Z. Cakir, F. Reichenbach, F. Emschermann, J. Lauterwasser, A. Kaiser, G. Ichim, S.W. Tait, S. Frank, H.F. Langer, F. Edlich, Differential retrotranslocation of mitochondrial Bax and Bak, EMBO J. 34 (2015) 67–80, https://doi.org/10.15252/embj.201488806.

[28] R.T. Uren, M. O'Hely, S. Iyer, R. Bartolo, M.X. Shi, J.M. Brouwer, A.E. Alsop, G. Dewson, R.M. Kluck, Disordered clusters of Bak dimers rupture mitochondria during apoptosis, Elife 6 (2017), https://doi.org/10.7554/eLife.19944.

[29] A.J. Valentijn, A.P. Gilmore, Translocation of full-length bid to mitochondria during anoikis, J. Biol. Chem. 279 (2004) 32848–32857, https://doi.org/10.1074/jbc.M313375200.

[30] J. Zhang, F. Lin, L. Chai, L. Wei, T. Chen, Iiem-Spfret: improved Iem-Spfret method for robust Fret measurement, J. Biomed. Opt. 21 (2016) 105003, , https://doi.org/10.1117/1.JBO.21.10.105003.

[31] M.G. Erickson, B.A. Alseikhan, B.Z. Peterson, D.T. Yue, Preassociation of calmodulin with voltage-gated Ca2+ channels revealed by Fret in single living cells,

Neuron 31 (2001) 973–985, https://doi.org/10.1016/S0896-6273(01)00438-X.
[32] A. Hoppe, K. Christensen, J.A. Swanson, Fluorescence resonance energy transfer-based stoichiometry in living cells, Biophys. J. 83 (2002) 3652–3664, https://doi.org/10.1016/S0006-3495(02)75365-4.
[33] T. Zal, N.R. Gascoigne, Photobleaching-corrected Fret efficiency imaging of live cells, Biophys. J. 86 (2004) 3923–3939, https://doi.org/10.1529/biophysj.103.022087.
[34] A. Nechushtan, C.L. Smith, I. Lamensdorf, S.H. Yoon, R.J. Youle, Bax and Bak coalesce into novel mitochondria-associated clusters during apoptosis, J. Cell Biol. 153 (2001) 1265–1276, https://doi.org/10.1083/jcb.153.6.1265.
[35] L. Zhou, D.C. Chang, Dynamics and structure of the Bax-Bak complex responsible for releasing mitochondrial proteins during apoptosis, J. Cell Sci. 121 (2008) 2186–2196, https://doi.org/10.1242/jcs.024703.
[36] Emily H.Y.A. Cheng, Michael C. Wei, Solly Weiler, Richard A. Flavell, Tak W. Mak, Tullia Lindsten, Stanley J. Korsmeyer, Bcl-2, Bcl-Xl sequester Bh3 domain-only molecules preventing Bax- and Bak-mediated mitochondrial apoptosis, Mol. Cell 8 (2001) 705–711, https://doi.org/10.1016/s1097-2765(01)00320-3.
[37] S.N. Willis, L. Chen, G. Dewson, A. Wei, E. Naik, J.I. Fletcher, J.M. Adams, D.C. Huang, Proapoptotic Bak is sequestered by Mcl-1 and Bcl-Xl, but not Bcl-2, until displaced by Bh3-only proteins, Genes Dev. 19 (2005) 1294–1305, https://doi.org/10.1101/gad.1304105.
[38] F. Todt, Z. Cakir, F. Reichenbach, R.J. Youle, F. Edlich, The C-terminal helix of Bcl-X (L) mediates Bax retrotranslocation from the mitochondria, Cell Death Differ. 20 (2013) 333–342, https://doi.org/10.1038/cdd.2012.131.
[39] E.H. Cheng, T.V. Sheiko, J.K. Fisher, W.J. Craigen, S.J. Korsmeyer, Vdac2 inhibits Bak activation and mitochondrial apoptosis, Science 301 (2003) 513–517, https://doi.org/10.1126/science.1083995.
[40] M. Lazarou, D. Stojanovski, A.E. Frazier, A. Kotevski, G. Dewson, W.J. Craigen, R.M. Kluck, D.L. Vaux, M.T. Ryan, Inhibition of Bak activation by Vdac2 is dependent on the Bak transmembrane anchor, J. Biol. Chem. 285 (2010) 36876–36883, https://doi.org/10.1074/jbc.M110.159301.
[41] N. Popgeorgiev, L. Jabbour, G. Gillet, Subcellular localization and dynamics of the Bcl-2 family of proteins, Front. Cell Dev. Biol. 6 (2018) 13, https://doi.org/10.3389/fcell.2018.00013.
[42] C. Sheridan, P. Delivani, S.P. Cullen, S.J. Martin, Bax- or Bak-induced mitochondrial fission can be uncoupled from cytochrome C release, Mol. Cell 31 (2008) 570–585, https://doi.org/10.1016/j.molcel.2008.08.002.
[43] P.S. Jeng, A. Inoue-Yamauchi, J.J. Hsieh, E.H. Cheng, Bh3-dependent and independent activation of Bax and Bak in mitochondrial apoptosis, Curr. Opin. Physiol. 3 (2018) 71–81, https://doi.org/10.1016/j.cophys.2018.03.005.
[44] S.Y. Jeong, B. Gaume, Y.J. Lee, Y.T. Hsu, S.W. Ryu, S.H. Yoon, R.J. Youle, Bcl-X(L) sequesters its C-terminal membrane anchor in soluble, cytosolic homodimers, EMBO J. 23 (2004) 2146–2155, https://doi.org/10.1038/sj.emboj.7600225.
[45] A. Aranovich, Q. Liu, T. Collins, F. Geng, S. Dixit, B. Leber, D.W. Andrews, Differences in the mechanisms of proapoptotic Bh3 proteins binding to Bcl-xl and Bcl-2 quantified in live Mcf-7 cells, Mol. Cell 45 (2012) 754–763, https://doi.org/10.1016/j.molcel.2012.01.030.
[46] S. Bleicken, A. Hantusch, K.K. Das, T. Frickey, A.J. Garcia-Saez, Quantitative interactome of a membrane Bcl-2 network identifies a hierarchy of complexes for apoptosis regulation, Nat. Commun. 8 (2017) 73, , https://doi.org/10.1038/s41467-017-00086-6.
[47] J.M. Bowen, R.J. Gibson, A.G. Cummins, D.M. Keefe, Intestinal mucositis: the role of the Bcl-2 family, P53 and caspases in chemotherapy-induced damage, Support Care Cancer 14 (2006) 713–731, https://doi.org/10.1007/s00520-005-0004-7.
[48] M.Y. Du, F.F. Yang, Z.H. Mai, W.F. Qu, F.R. Lin, L.C. Wei, T.S. Chen, Fret two-hybrid assay by linearly fitting Fret efficiency to concentration ratio between acceptor and donor, Appl. Phys. Lett. 112 (2018) 153702, , https://doi.org/10.1063/1.5021466.
[49] G. Dewson, T. Kratina, H.W. Sim, H. Puthalakath, J.M. Adams, P.M. Colman, R.M. Kluck, To trigger apoptosis, Bak exposes its Bh3 domain and homodimerizes via Bh3:groove interactions, Mol. Cell 30 (2008) 369–380, https://doi.org/10.1016/j.molcel.2008.04.005.
[50] D. Westphal, R.M. Kluck, G. Dewson, Building blocks of the apoptotic pore: how Bax and Bak are activated and oligomerize during apoptosis, Cell Death Differ. 21 (2014) 196–205, https://doi.org/10.1038/cdd.2013.139.
[51] G. Dewson, T. Kratina, P. Czabotar, C.L. Day, J.M. Adams, R.M. Kluck, Bak activation for apoptosis involves oligomerization of dimers via their Alpha6 helices, Mol. Cell 36 (2009) 696–703, https://doi.org/10.1016/j.molcel.2009.11.008.
[52] T. Mandal, S. Shin, S. Aluvila, H.C. Chen, C. Grieve, J.Y. Choe, E.H. Cheng, E.J. Hustedt, K.J. Oh, Assembly of Bak homodimers into higher order homo-oligomers in the mitochondrial apoptotic pore, Sci. Rep. 6 (2016) 30763, , https://doi.org/10.1038/srep30763.
[53] K. Cosentino, A.J. Garcia-Saez, Bax and Bak pores: are we closing the circle? Trends Cell Biol. 27 (2017) 266–275, https://doi.org/10.1016/j.tcb.2016.11.004.